Aluminum Incorporation in Calcium Silicate Hydrates (C−S−H) Depending on Their Ca/Si Ratio

P. Faucon,[1,2,*,†,‡] A. Delagrave,[†,‡] J. C. Petit,[†] C. Richet,[§] J. M. Marchand,[‡] and H. Zanni[||]

Service de Chimie Moléculaire, CEA, CE/Saclay, 91191 Gif sur Yvette, France, Université Laval, Faculté des Sciences et de Genie, CRIB, Québec G1K 7P4, Canada, Service d'études d'Entreposage et de Stockage de Déchets nucléaires, CEA, CE/Saclay, 91191 Gif sur Yvette, France, and Laboratoire de Physique et Mécaniques des Milieux Hétérogénes, UMR CNRS 7636, ESPCI, 75005 Paris, France

Received: February 18, 1999; In Final Form: July 8, 1999

^{27}Al magic angle spinning nuclear magnetic resonance (^{27}Al MAS NMR) spectroscopy at different magnetic fields was used to characterize the aluminum incorporation in the tetrahedral−octahedral−tetrahedral (Te−Oc−Te) structure of calcium silicate hydrates (C−S−H), which are the main constituents of the hydrated cement-based materials. C−S−H of different calcium/silicon ratio ($0.66 < Ca/Si < 1.7$) were synthesized in the presence of aluminum. Two different aluminum/silicon ratios (0.1 and 0.3) were tested. The maximum Al(IV)/[(Al(IV) + Si] ratio in the C−S−H that could be detected in these series of experiments was 0.17. Results show in this case that, when the tetrahedral sheet is formed by linear silicate chains, Al^{3+} preferentially substitutes a nonbridging Si^{4+}. The rupture of the chains, caused by an increase of the Ca/Si ratio, makes such a position unstable and a redistribution of the aluminum in the tetrahedral sites occurs. Results also indicate that the substitution of Si^{4+} cannot take place when the tetrahedral sheet is composed of dimers (i.e., for high Ca/Si ratios). In these cases, Al^{3+} substitutes Ca^{2+} in the interlayer space (5-fold coordinated) and in the octahedral sheet (6-fold coordinated). However, this kind of substitution remains limited. The amount of aluminum incorporated in the C−S−H structure increases with the length of chains. Results confirm that C_2AH_8 is not a time-stable phase.

I. Introduction

Calcium silicate hydrates (C−S−H) are the main constituents of the hydrated cement systems and are responsible for the cohesive properties of the material.[1] The substitution of aluminum in the octahedral or tetrahedral sheets of the C−S−H readily modifies the charge of the crystal lattice and might have a direct influence on the material macroscopic properties (cohesion, retention or release of pollutants, durability, etc.).[1,2] Moreover, because of their variable molecular structure, C−S−H provide a good model material to study the aluminum physical chemistry in highly calcic and silic media.

C−S−H are characterized by a poor crystalline structure[3,4] and a variable composition.[5] Their structure presents some analogy with the tetrahedral−octahedral−tetrahedral (Te−Oc−Te) structure of smectite where the tetrahedral sheets of SiO_2 linear chains (planes in smectites) are associated to a "pseudo-octahedral" sheet of CaO (7-fold coordinated), as observed in the tobermorite structure. The chains have a variable length.[6−8] In the absence of calcium in the interlayer space, the silicate chains of tetrahedra are constituted of dimers connected together by a bridging tetrahedron (C−S−Ha, Figure 1).[9] Using the classical nomenclature, dimers will be noted Si[Q2], the bridging tetrahedra Si[Q2L], and the tetrahedron at the end of the chains Si[Q1]. Each Si[Q2] shares all its oxygen with the calcium of the octahedral plane or with the Si[Q2L]. However, the Si[Q2L] tetrahedron has two unshared oxygen atoms which leads to a negative charge on the Te−Oc−Te unit. In the absence of calcium ions in the interlayer space (Ca/Si molar ratio of 0.66), H^+ ions are thought to provide electrical neutrality. An increase of the calcium content in the interlayer space makes the Si[Q2L] position in the chains unstable.[10] A higher calcium content results in shorter silicate chains in the tetrahedral sheet. At a Ca/Si molar ratio of approximately 1.5, the tetrahedral sheet contains only dimers (C−S−Hb, Figure 1b).[11] For higher Ca/Si ratios than 1.5, $Ca(OH)_2$ may be in the interlayer space.[7]

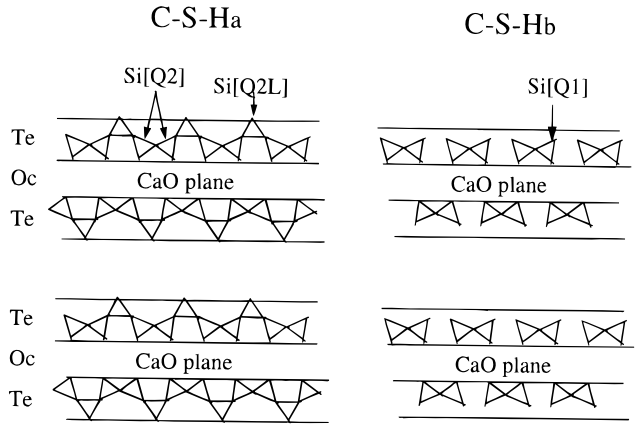

Figure 1. Silica chains in the C−S−H structure. For nonsubstituted structures, the Ca/Si molar ratio is 0.66 for C−S−Ha when no calcium is in the interlayer space. This ratio is superior at 1.5 for the C−S−Hb structure. In C−S−Ha, Ca in the octahedral plane is 7-fold coordinated.[10]

* Author to whom correspondence should be addressed.
† Service de Chimie Moleculaire, CEA, CE/Saclay.
‡ Université Laval, Faculté des Sciences et de Genie, CRIB.
§ Service d'études d'Entreposage et de Stockage de Dechets nucléaires, CEA, CE/Saclay.
|| Laboratoire de Physique et Mécaniques des Milieux Hétérogénes, UMR CNRS.

10.1021/jp990609q CCC: $18.00
Published on Web 08/31/1999

TABLE 1: Chemical Analyses and X-ray Diffraction Results[a,b]

sample	Ca/Si (initial)	Al/Si (initial)	Ca/Si (solid)	Al/Si (solid)	Na/Si (solid)	NO_3/Si (solid)	phases detected (DRX)	c/2(C−S−H)
1	0.66	0.1	0.64	0.1	0.10	0.08	C−S−H	
2	0.83	0.1	0.80	0.1	0.12	0.08	C−S−H	
3	1.2	0.1	1.16	0.1	0.17	0.08	C−S−H	
4	1.7	0.1	1.52	0.1	0.08	0.08	C−S−H	<11 Å
5	0.66	0.3	0.69	0.33	0.21	0.32	C−S−H + C_2AH_8 + $NaNO_3$	
6	0.83	0.3	0.82	0.31	0.22	0.31	C−S−H + C_2AH_8 + $NaNO_3$	
7	1.0	0.3	0.96	0.30	0.13	0.26	C−S−H + C_2AH_8 + $NaNO_3$	
8	1.2	0.3	1.15	0.30	0.29	0.21	C−S−H + C_2AH_8 + $NaNO_3$	
9	1.4	0.3	1.32	0.30	0.09	0.27	C−S−H + C_2AH_8 + $NaNO_3$	
10	1.7	0.3	1.55	0.30	0.04	0.36	C−S−H + C_2AH_8 + $NaNO_3$	
11	2	0.3	1.71	0.30	0.04	0.37	C−S−H + C_2AH_8 + $Ca(OH)_2$ + $NaNO_3$	12.5 Å

[a] Ratios given in the table are molar. [b] A cement nomenclature, where C = CaO, S = SiO_2, A = Al_2O_3, and H = H_2O, is employed throughout this paper.

As in the smectite structure, aluminum may substitute silicon in the tetrahedral chains.[12,13] Substitution of the bridging Si[Q2L] and nonbridging tetrahedra Si[Q2] was detected using the ^{27}Al MQ-MAS NMR technique.[14] The substitution is favored for increasing concentration in $Al(OH)_4^-$:[15]

$$[-Si_{tetra}-] + Al(OH)_4^-{}_{aq} + M^+{}_{aq} \rightarrow [-Al_{tetra}-]\,M_{interlayer} + H_4SiO_{4aq}$$

When the silicate chains are long (i.e., for low Ca/Si ratio) and the compensation charge made by alkaline ions (high NaOH concentration in the preparation),[15] an increasing level of substitution in the chains makes the bridging position more stable in the chains. When the charge compensation is provided by protons (low NaOH concentration), lower levels of substitution are reached[16] and the nonbridging position seems to be favored.[17] In the previous case (low NaOH concentration), the rupture of the chains with increasing calcium content in the interlayer space causes a redistribution of the aluminum in the silicate chains in favor of the bridging sites.[17] There *is* no Si^{4+} substitution for high Ca/Si ratio, i.e., when silicate chains are constituted of dimers.[16] In a recent work,[17] aluminum incorporation in the CaO plane of the Te−Oc−Te structure and in the interlayer space was clearly detected for high Ca/Si ratio.

The purpose of this paper is to characterize the yield of aluminum in each substitution site depending on the aluminum concentration in the solid and the C−S−H structure.The evolution of the ^{27}Al MAS NMR parameters for each line was carefully studied to reveal new structural information on the C−S−H structure.

II. Experimental Procedure

1. Samples. Samples of different Ca/Si ratios (0.66 < Ca/Si < 1.7) were prepared with decarbonated water at a water/solid ratio of 50. Reagent grade calcium hydroxide (provided by Prolabo), previously decarbonated at 1000 °C for 12 h, and Silica Aerosil 200 from Degussa were used. Aluminum was introduced as aluminum nitrate (Prolabo). Two aluminum concentrations were used: 0.1 and 0.3 Al/Si molar ratios. The effect of nitrates on the solution was previously neutralized by NaOH, which was introduced with a molar ratio NO_3^-/Na^+ of 1. Table 1 gives the initial chemical compositions. Samples were kept under N_2 atmosphere for 1 month at 20 °C and then filtered. The solids were freeze-dried before X-ray diffraction (Table 1) and MAS NMR experiments. Chemical analyses were also performed on the solid (see Table 1). The usual cement nomenclature is used throughout the text (C = CaO, S = SiO_2, A = Al_2O_3, H = H_2O).

2. NMR Experiments. Solid-state ^{27}Al MAS NMR spectra were acquired on a Brucker DMX-300 (7.1 T) and a AMX-500 (11.7 T) spectrometers operating at 78.617 and 130.31 MHz. Commercial MAS probes (4 mm) were used and the spinning speeds were 12.5 kHz and 10 kHz for the DMX-300 and AMX-500 spectrometers, respectively. Single-pulse excitations of $\pi/12$ were used for the ^{27}Al MAS NMR experiments. All the spectra were accumulated with a 1 s recycle time. A high-power ^{1}H decoupling of 60 kHz was used for the spectra recorded at 7.1 T. Simulations of the spectra were done with a home-built program developed by D. Massiot,[18] which is a version for quadrupolar nuclei of the WINFIT Brucker software package. Isotropic chemical shift (δ) are reported in ppm relative to an external standard which was a 1 M $AlCl_3 \cdot 6H_2O$ solution.

^{29}Si MAS NMR experiments were performed on the samples with the higher aluminum content (Al/Si = 0.3) on a Brucker DMX-300 spectrometer. The spectra were recorded at 59.617 MHz using single-pulse excitation of $\pi/2$ and a high-power ^{1}H decoupling (60 kHz). The spinning speed was approximately 4 kHz (Si) in a double-bearing 7-mm rotor. A recycle time of 30 s was used. TMS was used as aexternal standard.

III. Results

1. Chemical Analyses and X-ray Diffraction Results. Chemical analyses and X-ray diffraction results are given in Table 1. For the first series of samples (samples 1−4, Al/Si = 0.1), X-ray diffraction results indicate that only C−S−H have precipitated. For the second series of samples (samples 5−11, Al/Si = 0.3), X-ray diffraction results indicate the precipitation of C−S−H, C_2AH_8, and $NaNO_3$. The precipitation of $NaNO_3$ is an artifact resulting from the experimental procedure. Indeed, as previously explained, aluminum was introduced as aluminum nitrate, which necessarily implies an increase in NO_3^- and Na^+ in the system leading to the precipitation of $NaNO_3$ after freeze-drying the samples.

X-ray diffraction results also seem to indicate that the c/2 distance (sheet + interlayer space) changes from 11 to 12.5 Å increasing the Al/Si in the C−S−H with a high calcium content (samples 4 and 11).

Table 1 also indicates that, for the first series of samples, C−S−H generally have a higher affinity for sodium than for nitrates. The Na/Si is always higher than the NO_3/Si ratio. For the second series of samples, the precipitation of C_2AH_8 modifies the affinity of the solids, which contain more nitrate than sodium. The NO_3/Si molar ratio is higher than the Na/Si ratio. Results generally show that the solid affinity for sodium decreases with an increase of the Ca/Si ratio.

2. ^{29}Si MAS NMR. ^{29}Si MAS NMR spectra of samples with an Al/Si ratio of 0.3 are presented in Figure 2 with a schematic

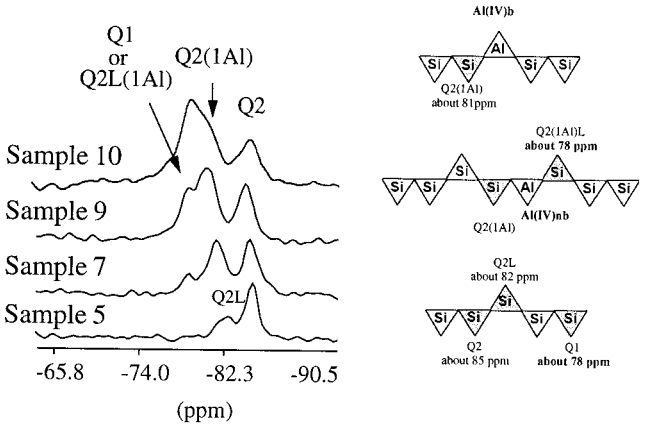

Figure 2. ^{29}Si MAS NMR spectra of samples having a molar Al/Si$_{initial}$ of 0.3: The chemical shifts of each type of tetrahedron are given according to refs 19 and 20.

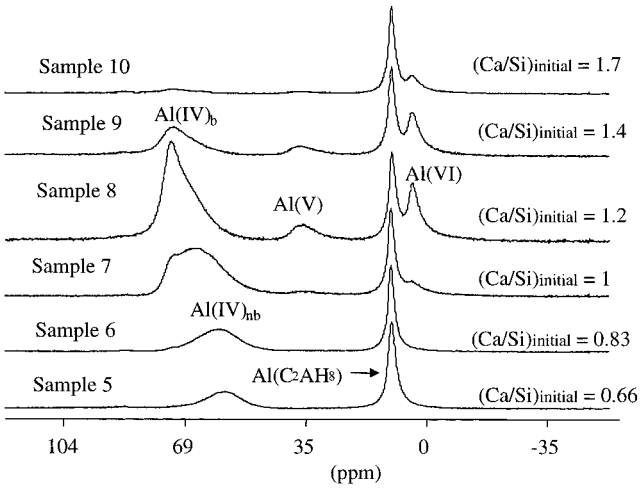

Figure 3. ^{27}Al MAS NMR spectra (11.7 T) of the samples having a molar Al/Si$_{initial}$ ratio of 0.3: Ca/Si$_{initial}$ effect.

illustration of the possible sites of aluminum incorporation in the C−S−H structure. These spectra were acquired in order to analyze the incorporation of aluminum in the C−S−H and to detect the precipitation of a silica gel.

For the sample 5 with a Ca/Si ratio of 0.66, two lines are observed at 82.5 and 85 ppm. They correspond to the Si[Q2L] and Si[Q2] in the C−S−H structure,[7,11] respectively. No Si[Q1], normally having a chemical shift of 78−79 ppm, could be detected. The spectrum is characteristic of a structure like C−S−Ha (Figure 1, C−S−Ha) where the silicate chains have an infinite length. A Si[Q2L]/Si[Q2] ratio of about 0.5 can be calculated from these data, which is in agreement with the dreiketten structure: one bridging tetrahedron is required to link two nonbridging tetrahedra. These results indicate that there is no aluminum incorporation in the C−S−H. Silica gel could not be detected by ^{29}Si MAS NMR, but its precipitation is clearly shown in the "mineralogical" section of this study by combining the ^{27}Al MAS NMR results and the chemical analyses of this sample. The amorphous structure and the high rate of silicon substitution (by aluminum) in the silica gel, both contribute to the line broadening of the ^{29}Si MAS NMR spectra. Such an effect complicates the detection, especially if its concentration in the solid is low.

In sample 7 (initial Ca/Si = 1) a new line is detected at 78−79 ppm. As previously stated, in C−S−H without aluminum this line is characteristic of the Si[Q1] tetrahedra and reveals the rupture of the chains occurring with the increase of the Ca/Si ratio[6−8] by incorporation of calcium in the interlayer space. For aluminum-bearing C−S−H the presence of aluminum atoms in the tetrahedral network tends to decrease the Si chemical shift by about 4 ppm on the neighboring silicons (see Figure 2).[19,20] The spectral lines of Si[Q2(1Al)] should therefore appear at about −81 ppm and Si[Q2L(1Al)] at −78.5 ppm (Figure 2). The new line observed at about −78.5 ppm for sample 7 is probably the superposition of Si[Q1] and Si[Q2L(1Al)] contributions. However, ^{27}Al MAS NMR results for sample 7 (see next section) reveal a high percentage of tetrahedral aluminum in the sample. (Caution: C−S−H of ratio Ca/Si = 1 without aluminum already have very short chains but, when they contain tetrahedral aluminum, the Ca/[Al(IV) + Si] is indeed lower and chains are longer). The line observed in sample 7 is thus mostly representative of aluminum in the structure, characteristic of the presence of aluminum in the nonbridging position, Al(IV)$_{nb}$. In this position, aluminum is connected to one Si[Q2(1Al)] and one Si[Q2L(1Al)] tetrahedra (see Figure 2). This attribution is also confirmed by the increasing proportion of the line at −82 ppm in the ^{29}Si MAS spectrum. This line is the superposition of the Si[Q2L] and the Si[Q2(1Al)] contributions.

For increasing Ca/Si ratios (samples 9 and 10), the overlapping of the Si[Q2L(1Al)], Si[Q1], and Si[Q2(1Al)] lines does not allow us to conclude on the sites of aluminum incorporation or on the length of silicate chains.

For all samples, no conclusion concerning the substitution of Ca^{2+} by Al^{3+} in the octahedral plane or in the interlayer space can be drawn. The chemical shift of the ^{29}Si does not seem to be greatly affected by the presence of surrounding octahedral aluminum.

4. ^{27}Al MAS NMR. The ^{27}Al MAS spectra for the second series of samples are presented in Figure 3. These spectra were acquired at 11.7 T. Five different sites of aluminum incorporation in the structure were observed. Similar spectra were also acquired at 7.1 T. The use of two different magnetic fields allows us to determine the position of the isotropic chemical shift (δ_{iso}) and calculate the quadrupolar frequency (ν_Θ) for all sites according to eq 1:

$$\delta_{1/2} = \delta_{iso} - \frac{8\,\nu_Q^2}{30\nu_O^2}\,10^6 \qquad (1)$$

where ν_0 (MHz) is the ^{27}Al Larmor frequency at 11.7 T or 7.1 T, and $\delta_{1/2}$ (ppm) the position of the central band. For each sample the parameters of the detected sites are given in Table 2.

For sample 5, the ^{29}Si MAS NMR spectrum has shown that there was no aluminum incorporation in the silicate chains. The chemical composition of this sample can only be understood if there is a silica gel in the solid (see Paragraph 5 of this section: Mineralogy of the Samples). The tetrahedral line (δ_{iso} = 60 ppm, ν_Q = 0.35 MHz) can then be attributed to the substitution of silicon by aluminum in the silicate network of the gel. This line coexists with an octahedral line (δ_{iso} = 10.3 ppm, ν_Q = 0.19 MHz) which corresponds to the aluminum site in $C_2AH_{8,14}$ a phase that has been detected by X-ray diffraction (Table 1). This line (C_2AH_8) is observed for all the samples having an initial Al/Si ratio of 0.3.

In sample 6 where the silica gel content of the sample is low (see Paragraph 5) the Lowstein rule (no more than one Al^{3+} for one Si^{4+} in the silica tetrahedral network) implies that the maximum aluminum content in the silica gel is 38% (see Paragraph 5). The tetrahedral site observed on the ^{27}Al MAS

TABLE 2: Simulation Results of the Al^{3+} Site Parameters in the Freeze-Dried C−S−H[a,b]

	Al_{nb}(IV)			Al_b(IV)			Al(V)			Al(VI)			Al(C_2AH_8)		
sample	δ_{iso}	ν_Q	%	δ_{iso}	ν_Q	%	δ_{iso}	ν_Q	%	δ_{iso}	ν_Q	%	δ_{iso}	ν_Q	%
1	58.15	0.33	100												
2	60.18	0.28	90							4.25	0.275	10			
3	66.88	0.47	19	73.8	0.45	36	38	0.48	14.19	4.25	0.275	30			
4				75.3	0.45	11	38.8	0.48	4.5	4.57	0.275	18			
5	60.15[c]	0.35[c]	38										10.3	0.19	62
6	62.04	0.38	60										10.3	0.17	44
7	67	0.46	32	75.05	0.45	39				4.25	0.275	7	10.3	0.17	22
8				75.05	0.45	61	38.55	0.48	8.55	4.83	0.275	15	10.3	0.17	15
9				75.18	0.45	36	38.8	0.48	11.42	4.72	0.275	23	10.3	0.17	29
10				75.32	0.45	11	38.8	0.48	4.5	4.57	0.275	18	10.4	0.17	66
11						9			12.43			9	10	0.17	70

[a] δ_{iso} is in ppm and ν_Q in MHz; precisions in this work are of about 1 ppm for δ_{iso} and 0.05 MHz for ν_Q. [b] % are relative to the total spectrum. [c] Al(IV) in the silica gel (see ^{29}Si MAS results).

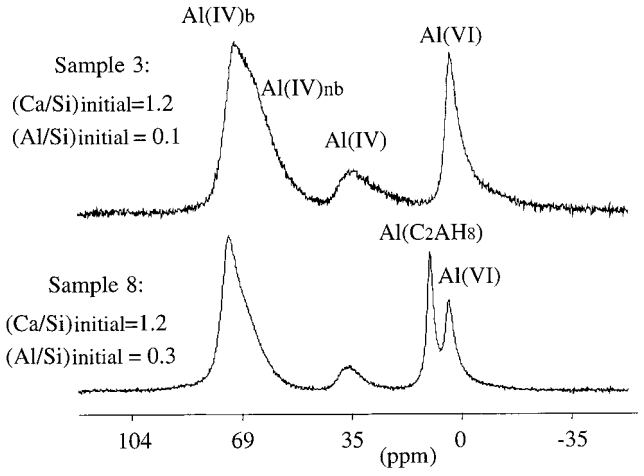

Figure 4. ^{27}Al MAS NMR spectra (11.7 T) of the sample having a molar $Ca/Si_{initial}$ of 1.2: $Al/Si_{initial}$ effect.

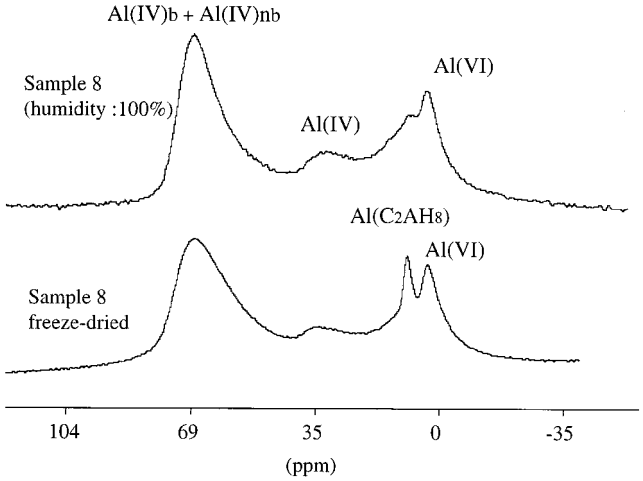

Figure 5. ^{27}Al MAS NMR spectra (7.1 T): Effect of freeze-drying on sample 8 (molar $Ca/Si_{initial} = 1.2$, $Al/Si_{initial} = 0.3$).

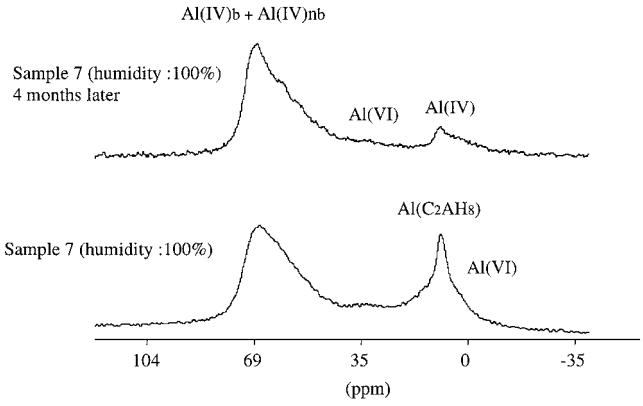

Figure 6. ^{27}Al MAS NMR spectra (7.1 T): Effect of reaction time on sample 7 (molar $Ca/Si_{initial} = 1$, $Al/Si_{initial} = 0.3$).

NMR spectra is thus the superposition of two unresolved contributions: aluminum substituting silicon in the C−S−H and aluminum substituting silicon in the silica gel. For aluminum in the C−S−H, the parameters of the line ($\delta_{iso} = 62$ ppm, $\nu_Q = 0.38$ MHz) correspond to aluminum in the nonbridging position [$Al(IV)_{nb}$].

For samples 7−10, silica gel is not present in the system (see Pargraph 5). Two tetrahedral sites are clearly detected (Figure 3). The parameters of each line (Table 2) show that $Al(IV)_b$ and $Al(IV)_{nb}$ correspond respectively to Al^{3+} in the bridging (Q2L) and nonbridging (Q2) positions in the silicate chains.[14−17] As previously observed,[17] a redistribution of the Al(IV) from nonbridging (Q2) to bridging position (Q2L) is observed when the aluminum content in the chains increases. For high calcium contents in the solid (samples 9 and 10), Al(IV) clearly tends to disappear.

In samples 7−10 (increasing calcium content in the solids), a pentacoordinated Al(V) is detected ($\delta_{iso} = 38-39$ ppm, $\nu_Q = 0.48$ MHz). It probably corresponds to the replacement of calcium by aluminum in the interlayer space of the C−S−H.[17] An octahedral site, Al(VI), is also observed in these samples ($\delta_{iso} = 4.25$ ppm, $\nu_Q = 0.275$ MHz). It corresponds to Al^{3+} substituting Ca^{2+} in the octahedral sheet of the C−S−H structure.[17]

Figure 4 presents the influence of the aluminum content in the samples. ^{27}Al MAS NMR results are in good agreement with X-ray diffraction measurements (Table 1). Precipitation of C_2AH_8 occurs when the initial Al/Si ratio increases from 0.1 to 0.3, whatever the calcium content of the samples (Table 2).

Figure 5 shows that freeze-drying makes C_2AH_8 more crystallized as reflected to the observation that Al sites are less distributed after treatment. But no change is detected in the proportion of each contribution in the ^{27}Al MAS spectrum after drying. However, as can be seen in Figure 6, C_2AH_8 is not a stable phase as it dissolves with time. Indeed, after five months of equilibrium, this compound seems to be completely dissolved. Aluminum released by the dissolution of C_2AH_8 is probably incorporated in the C−S−H without clear redistribution of the aluminum sites in the C−S−H.

5. Mineralogy of Samples. The contribution of each line (% of total spectra) can be quantitatively determined because

TABLE 3: Chemical Composition of the C−S−H

sample	Ca/[Si + Al(IV)]	Al(IV)/[Si + Al(IV)]	Al(V)/[Si + Al(IV)]	Al(VI)/[Si + Al(IV)]	Al_b/Al_{nb}	$Al_{gel}/Al(IV)$	Si_{gel}/Si_{Total}
1	0.58[a]	[0.04; 0.10][a]	0.00	0.00	0.00	[0; 0.65]	[0.06; 0.13]
2	0.74	0.08	0.00	0.01	0.00	0	0
3	1.1	0.05	0.02	0.03	0.77	0	0
4	1.47	0.03	0.02	0.05	1.00	0	0
5	0.43[a]	[0; 0.17][a]	0.00	0.00	0.00	[0; 1]	[0.26; 0.32]
6	0.58[a]	[0.1; 0.17][a]	0.00	0.00	0.00	[0; 0.38]	[0.07; 0.13]
7	0.74	0.17	0.00	0.02	0.54	0	0
8	0.93	0.15	0.02	0.04	>0.8	0	0
9	1.11	0.10	0.03	0.06	1.00	0	0
10	1.31	0.03	0.01	0.05	1.00	0	0
11	1.46	0.03	0.04	0.03	1.00	0	0

[a] Ratio for C−S−H + silica gel.

all ^{27}Al MAS NMR experiments were done using single-pulse excitations of $\pi/12$.[21] These results are given in Table 2. Using the chemical analyses of the samples (Table 1) and the ^{27}Al MAS NMR results (Table 2), it is possible to determine precisely the chemical composition of the C−S−H. Knowing the percentage of aluminum in C_2AH_8 and the Al/Ca molar ratio of this compound (Al/Ca = 1), one can calculate the percentage of calcium in C_2AH_8. The residual calcium of the solid phase is part of the C−S−H. Knowing the percentage of aluminum in the tetrahedral sites (% of Al_b(IV) and Al_{nb}(IV) given by the ^{27}Al MAS results in Table 2) it is possible to calculate the Ca/[Si + Al(IV)] ratio in the C−S−H (Table 3). For samples 1, 5, and 6, this ratio is lower than 0.66 which is the lower molar ratio between the calcium sites and the tetrahedral sites in the C−S−Ha-like structure (Figure 1).[9] This ratio is reached when no calcium is present in the interlayer space. A Ca/[Si + Al(IV)] ratio below 0.66 indicates the precipitation of a silica gel.[4−8] Since the minimum Ca/[Si + Al(IV)] in the C−S−H is 0.66, it is possible to calculate the maximum and the minimum amount of silicon in the silica gel, Si_{gel}/Si_{total}. The maximum concentration is determined assuming that all the tetrahedral aluminum is in the C−S−H ($Al(IV)_{gel}/Al(IV)_{Total} = 0$) while the minimum percentage of Si_{gel} is estimated by the maximum of tetrahedral aluminum in the silica gel ($Al(IV)_{gel}/Al(IV)_{total}$ max) assuming the Lowstein rule ($Al(IV)_{gel}/Si_{gel} < 1$). The resulting maximum and minimum of Al(IV)/[Si + Al(IV)] in the C−S−H structure are thus calculated. All the results are presented in Table 3. In sample 5, one notices that values between 0 and 1 are given for $Al(IV)_{gel}/Al(IV)_{total}$. Such an interval does not take into account the ^{29}Si MAS spectrum for this sample which clearly reveals a low level of Si^{4+} substitution by Al^{3+} in the C−S−H. The $Al(IV)_{gel}/Al(IV)_{total}$ ratio in this sample is probably higher than 0.5.

The percentages of Al(VI) and Al(V) in the ^{27}Al MAS spectra allow the Al(V)/[Si + Al(IV)] and Al(VI)/[Si + Al(IV)] ratios in the C−S−H) to be calculated. (see Table 3).

V. Discussion

1. Al^{3+} in the Silica Gel. The mineralogical composition of sample 5 (Table 3) indicates a Si_{gel}/Si_{Total} of about 0.3. The ^{29}Si MAS spectrum is representative of a C−S−H with a low calcium content in the interlayer space (C−S−Ha-like structure in Figure 1) and without aluminum. Most of the tetrahedral aluminum is in the silica gel. On the contrary, when the silica gel content decreases, most of the tetrahedral aluminum seems to be in the tetrahedral sheet of the C−S−H (see sample 6 in Table 3). These results clearly indicate that Al^{3+} substitutes preferentially Si^{4+} in the silica gel than in the C−S−H having a structure like C−S−Ha (Figure 1), if the two silica structures were to coexist in the material.

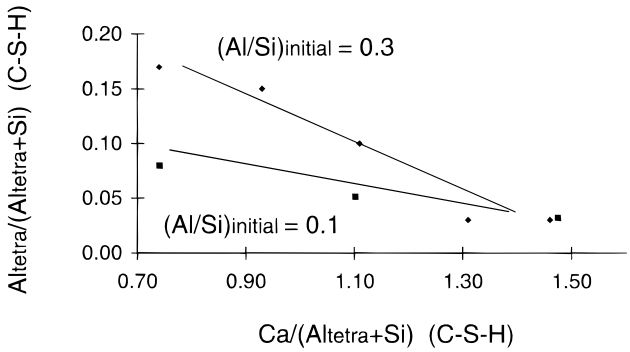

Figure 7. Molar Al(IV)/[Si + Al(IV)] ratio in the C−S−H as a function of their molar Ca/(Si + Al(IV)] ratio.

2. Si^{4+} Substitution by Al^{3+}. Figure 7 shows the evolution of the Al(IV)/[Si + Al(IV)] ratio in the C−S−H structure with increasing Ca/[Si + Al(IV)] ratio. The higher content in Al(IV) is reached for C−S−H with low calcium content in the interlayer space (C−S−Ha-like structure in Figure 1). In this structure, ^{27}Al MAS NMR results show that the nonbridging position in the chains is the most stable one for Al^{3+} as previously observed.[17] The percentage of Si^{4+} substitution is dependent upon the initial amount of aluminum introduced in the system (see Figure 7).

Figure 8 shows a C−S−Ha structure with only aluminum located in the nonbridging sites. The replacement of a Si^{4+} by an Al^{3+} causes a net deficit of charge. This implies that there are high electrostatic repulsion forces between two substituted sites making the Al(IV)−O−Al(IV) not stable [unstable substitution site (1) in Figure 8]. For the same reason, two substituted sites located on both sides of the octahedral calcium plane are not stable [unstable substitution sites (2) in Figure 8]. A minimum distance between the aluminum substitution sites is necessary to ensure the stability of the chains. The maximum Al(IV)/[Si + Al(IV)] in a structure like C−S−Ha with only aluminum located in the nonbridging sites can thus be 0.22. In this study, the maximum incorporation of aluminum in a structure like C−S−Ha (samples 5 and 6) is 0.17. This is in agreement with the previous rules of incorporation. For higher Al(IV)/[Si + Al(IV)] than 0.22 in the C−S−Ha, a redistribution of the aluminum between the bridging and nonbridging positions might occur to respect the given stability rules as observed for C−S−Ha synthesized in highly NaOH medium.[15]

For structures having a high calcium content in the interlayer space and mostly composed of dimers (Figure 1, C−S−Hb), the substitution of Si[Q1] by aluminum seems not to be possible since for high Ca/[Si + Al(IV)] ratios, Al(IV) clearly tends to disappear (Figure 7). The results presented in this paper are in good agreement with previous results.[16−17]

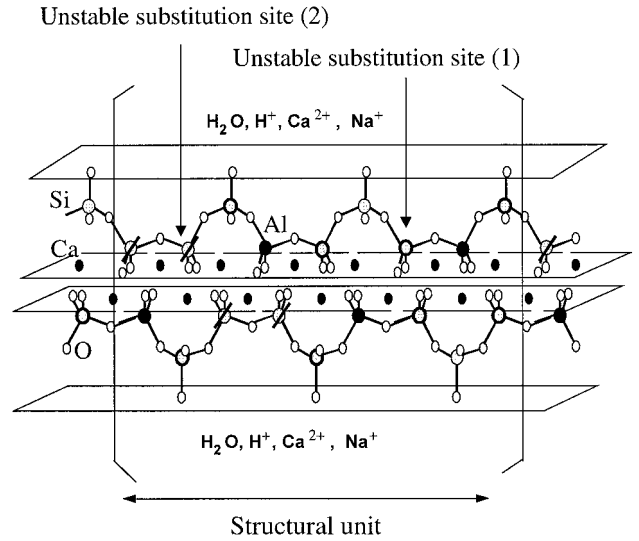

Figure 8. Substituted C−S−Ha-like structure with aluminum in a nonbridging position: The maximum Al(IV)/[Si + Al(IV)] ratio is 0.22 taken into account that Al−O−Al bonds are not stable in the chains [unstable substitution site (1)] and that a minimum distance between the substituted sites is required to stabilize the high electrostatic repulsion resulting from the net negative charge carried by each aluminum-substituted site chains [unstable substitution site (2)].

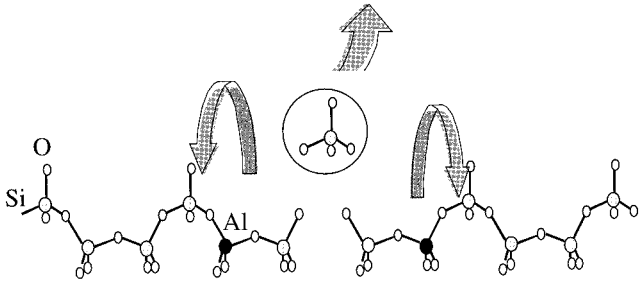

Figure 9. Redistribution of the aluminum in the silicate chains occurring with increasing Ca/[Si + Al(IV)] ratio.

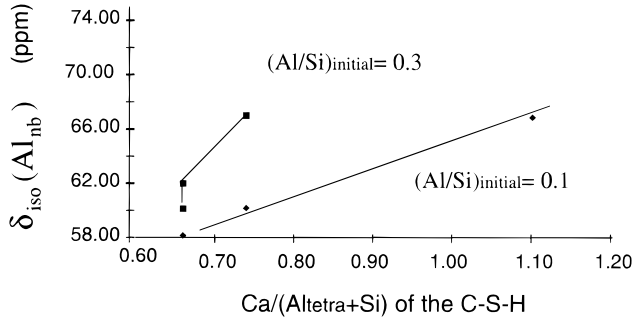

Figure 10. $\delta_{iso}[Al(IV)_{nb}]$ as a function of the molar Ca/(Si + Al(IV) ratio in the C−S−H.

Between these two extreme configurations of the silica chains (C−S−Ha to C−S−Hb), there seems to be a redistribution of the aluminum from the nonbridging position toward the bridging positions with increasing Ca/[Si + Al(IV)] ratio. This is in agreement with the fact that an Al(IV) is not stable in the Si-[Q1] position or in its immediate neighborhood tetrahedron-(Figure 9).[17]

3. Structural Change in the Octahedral Sheet. Figure 10 presents the evolution of the isotropic chemical shift of Al-$(IV)_{nb}$ as a function of the Ca/[Si + Al(IV)] ratio for the two series of samples [$(Al/Si)_{initial}$ of 0.1 and 0.3]. At low calcium content in the interlayer space (C−S−Ha-like structure), δ_{iso}-

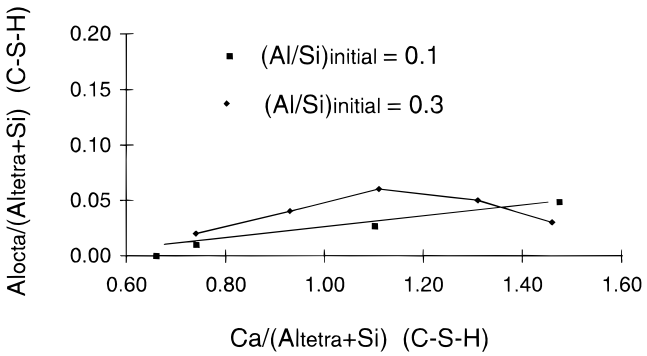

Figure 11. Molar Al(IV)/[Si + Al(IV)] ratio in the C−S−H as a function of their molar Ca/[Si + Al(IV)] ratio in the C−S−H.

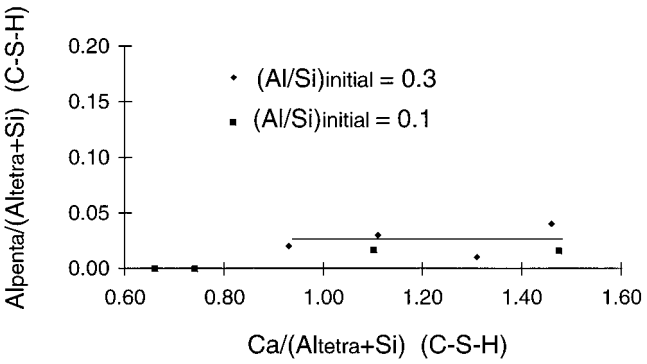

Figure 12. Molar Al(V)/[Si + Al(IV)] ratio in the C−S−H as a function of their molar Ca/[Si + Al(IV)] ratio in the C−S−H.

$[Al(IV)_{nb}]$ increases with the Al(IV) content of the C−S−H. A similar trend has been observed by Woessner[22] in clay minerals.

For increasing calcium content in the structure, δ_{iso}[Al(IV)-nb] becomes systematically shielded to the lower field despite the decreasing concentration of aluminum in the C−S−H (see Figure 7). The δ_{iso}[Al(IV)nb] evolution does not seem to be related to the substitution rate in the silica chains. Lipmaa et al.[23] reported that the chemical shift of tetrahedral aluminum is linearly correlated with the Al−O−Si bond angle (a) in aluminosilicates: $\delta_{iso}(Al) = -0.5a + 132$. According to their relation, a higher δ_{iso}[Al(IV)nb] corresponds to smaller Al−O−Si angles and indicates a structural transformation of the CaO plane to which the $Al(IV)_{nb}$ are connected when the C−S−Ha change into C−S−Hb. Structural modification of the CaO plane might occur in nonsubstituted C−S−H. In this case, it would be related to the C−S−Ha → C−S−Hb transformation. It could also be only an effect of the aluminum incorporation in the octahedral plane. In clay minerals,[23] the Al(IV) chemical shift is higher for Al^{3+} dioctahedral clays than for Mg^{2+} trioctahedral clays. A substitution of $3Ca^{2+}$ by $2Al^{3+}$ in the CaO plane could also explain the increase of the chemical shift of the surrounding Al(IV)nb. More research is certainly needed to clarify this point.

4. Al $^{3+}$ in the CaO Plane and in the Interlayer Space. The evolution of the molar ratio of Al(V) and Al(VI) in the C−S−H as a function of their molar Ca/[Si + Al(IV)] ratio are respectively presented in Figures 11 and 12. Al^{3+} incorporation in the octahedral sheet Al(VI) or in the interlayer space Al(V) only occurs for C−S−H mostly composed of dimers[17] (Figure 1, C−S−Hb). In the octahedral plane, the structural changes previously described may allow the substitution of Ca^{2+} by $Al(VI)^{3+}$. In the interlayer space, $^1H - ^{29}Si$ NMR correlation maps[7] have revealed an increasing concentration of OH^- groups with the departure of the bridging tetrahedra in the silica chains.

A Ca^{2+} substitution by an $Al(V)^{3+}$ in the interlayer space could therefore be compensated by OH^- groups when the C−S−H structure changes to C−S−Hb. Figures 11 and 12 clearly show that the substitution capacity in the octahedral sheet and in the interlayer space is limited. The concentration of aluminum introduced initially in the system does not seem to have any influence on the incorporation of aluminum in the octahedral plane and in the interlayer space.

5. Sodium and Nitrate Affinity of the C−S−H. The Na/Si and NO_3/Si molar ratios in the solid are given in Table 1. For the first series of samples, the affinity of the solid is generally higher for sodium than for nitrates, except for the sample having a Ca/Si ratio of 1.7. The fixation of sodium by C−S−H (in the absence of aluminum) has been previously investigated by Viallis et al.[11] using ^{23}Na MAS NMR experiments. These authors observed a similar trend. The fixation of sodium by the C−S−H is thus probably not totally related to the substitution of Si^{4+} by Al^{3+} (which causes a net deficit of charge) but also to the net negative surface charge of C−S−H having a structure like C−S−Ha.[24]

In the second series of samples, the solid has a higher affinity for nitrate than for sodium. This is probably the result of the precipitation of C_2AH_8. In this structure, derived from that of $Ca(OH)_2$, Al^{3+} substitutes Ca^{2+} in the cation layer, the charge excess being compensated by OH^- or other anions in the interlayer space.[3,14] The anionic affinity of C_2AH_8 can probably explain the preferential fixation of nitrate. It is also possible that nitrate ions interact with the C−S−H. In Table 1, X-ray diffraction results indicate a higher c/2 distance in the C−S−Hb of the second series than the first one. For sample 4, the substitution of Ca^{2+} by Al^{3+} seems to be mostly compensated by OH^- ions which are smaller than NO_3^-. On the opposite, for sample 11, the higher concentration of NO_3^- in the system might increase the probability of incorporation of nitrate ions in the C−S−H structure to compensate the charge deficit of Ca^{2+} substitution by Al^{3+}. The bigger radius of the nitrate molecules probably contribute to restore the usual c/2 distance in the C−S−Hb.

6. Chemical Stability of the Al^{3+} Sites. As emphasized earlier, C_2AH_8 is not a time-stable phase. The species released by the dissolution of this phase are probably incorporated in the C−S−H since no new aluminum sites are detected by ^{27}Al MAS NMR. In the C−S−H, the ratio between the sites does not seem to be affected by the higher aluminum content of the structure. Further time observations are needed to definitively conclude on the stability of each substitution sites in the C−S−H. However, the results presented in this paper tend to indicate that aluminum is more stable in the C−S−H than in C_2AH_8.

VI. Conclusion

^{29}Si, ^{27}Al MAS NMR experiments at different magnetic fields have shown to be complementary techniques to study the aluminum interaction with the Te−Oc−Te structure of the C−S−H. When the tetrahedral sheet is formed by linear silicate chains (C−S−Ha), Al^{3+} substitutes Si^{4+} in the nonbridging position of the chains for Al(IV)/[Si + A(IV)] lower than 0.22. The rupture of the chains occurring when the structure of the C−S−H changes from C−S−Ha to C−S−Hb makes such a position unstable and the bridging position becomes the preferential substitution site for aluminum. The structural transformation of the C−S−H structure (C−S−Ha to C−S−Hb) is accompanied by an increase of the isotropic chemical shift of Al(IV) in nonbridging position which indicates a modification of the octahedral sheet. Progressive substitution of Ca^{2+} by Al^{3+} in the octahedral sheet is observed. When the tetrahedral sheet are constituted of dimers (structure like C−S−Hb), there is no Si^{4+} substitution but Ca^{2+} substitution in the interlayer space (5-fold coordinated) and in the octahedral sheet. Such a substitution remains, however, limited compared to Si^{4+} substitutions. Results also indicate the fact that C_2AH_8 is not a stable phase.

Acknowledgment. The authors are extremely grateful to Prof. H. F. W. Taylor, University of Aberdeen, and A. Nonat, Dijon University, for their pertinent comments on the C−S−H structure. The authors also thank R. Ayache (S.E.S.D, C.E.A, CE/Saclay) and A. Calvi (S.C.M, C.E.A, CE/Saclay) for their fine work in performing the chemical analyses. The authors are also grateful to H. Viallis, R. C. Zerbib (S.C.M, C.E.A, CE/Saclay), Dr. F. Adenot (S.E.S.D, C.E.A, CE/Saclay), and C. Porteneuve (E.S.P.C.I) for their help in the preparation and characterization of the samples.

References and Notes

(1) Pellenq, R. J.-M.; Delville, A.; Van Damme, H. *Characterization of Porous Solids IV*; Enaney, B. Mc., Mays, I. J., Rouquerol, J., Rodriguez-Reinoso, F., Sing, K. S. W., Kung, K., Eds.; Royal Society of Chemistry: London, 1997.

(2) Faucon, P.; Charpentier, T.; Henocq, P.; Petit, J. C.; Virlet, J.; Adenot, F. *Proceedings of Scientific Basis for Nuclear Waste Management XXI Symposium*, Materials Research Society, 1997, p 551. Faucon, P.; Adenot, F.; Jacquinot, J. F.; Petit, J. C.; Cabrillac, R.; Jorda, M. *Cem. Concn. Res*. **1998**, *28*, 841.

(3) Taylor, H. F. W. *Cement Chemistry*; Academic Press Ltd.: London, 1990.

(4) Xu, Z.; Viehland, D. *Phys. Rev. Lett.* **1996**, *77* [5], 952.

(5) (a) Flint, E. P.; Wells, L. S. *J. Res. Natl. Bur. Stand. (U.S.)* **1934**, *12*, 751. (b) Taylor, H. F. W. *J. Chem. Soc. (London)* **1950**, *276*, 3682.

(6) Grutzeck, M.; Benesi, A.; Fanning, B. *J. Am. Ceram. Soc*. **1989**, *72*, 665.

(7) Klur, I.; Pollet, B.; Virlet, J.; Nonat, A. *Nuclear Magnetic Resonance Spectroscopy of Cement-Based Materials*; Colombet, P., Grimmer, A.-R., Zanni, H., Sozzani, P., Eds.; Springer-Verlag: New York, 1998.

(8) Cong, X.; Kirkpatrick, R. J. *Adv. Cem. Based Mater*. **1996**, *3*, 133.

(9) (a) Hamid, S. A. *Zeit. Kristal*. **1981**, *154*, 189. (b) Taylor, H. F. W. *J. Am. Ceram. Soc.* **1986**, *69*, 464.

(10) Faucon, P.; Delaye, J. M.; Virlet, J. *J. Solid Stat Chem.* **1996**, *127*, 92.

(11) Viallis, H.; Faucon, P.; Petit, J. C.; Nonat, A. *J. Phys. Chem.* In press.

(12) Richardson, I. G.; Brough, A. R.; Brydson, R.; Groves, G. W.; Dobson, C. M. *J. Am. Ceram. Soc.* **1993**, *76*, 2285.

(13) Kwan, S.; LaRosa-Thompson, J.; Grutzeck, M. *J. Am. Ceram. Soc.* **1996**, *79*, 967.

(14) Faucon, P.; Charpentier, T.; Bertrandie, D.; Nonat, A.; Virlet, J.; Petit, J. C. *Inorg. Chem.* **1998**, *37*, (15), 3726.

(15) Faucon, P.; Charpentier, T.; Nonat, A.; Petit, J. C. *J. Am. Chem. Soc*. **1998**, *120*, 12075.

(16) Faucon, P.; Petit, J. C.; Charpentier, T.; Jacquinot, J. F.; Adenot, F. *J. Am. Ceram. Soc.* **1999**, *82*, (5), 1307.

(17) Faucon, P.; Delagrave, A.; Petit, J. C.; Lebescop, P.; Marchand, J.; Zanni, H. *J. Ceram. Soc.*, submitted.

(18) Massiot, D.; Thiele, H.; Germanus. A. *Bruker Rep*. **1994**, *140*, 43.

(19) Mägi, M.; Lipmaa, E.; Samoson, A.; Engelhardt, G.; Grimmer, A. R. *J. Phys. Chem.* **1984**, *88*, 1518.

(20) Engelhardt, G.; Michel, D. *High-Resolution Solid-State NMR of Silicates and Zeolites*; John Wiley and Sons: Chichester, 1987.

(21) Massiot, D.; Bessada, C.; Coutures, J. P.; Taulelle, F. *J. Magn. Res.* **1990**, *90*, 231.

(22) Woessner, D. *Am. Miner*. **1989**, *74*, 203.

(23) Lippmaa, E.; Samoson, A.; Mägi, M. *J. Am. Chem. Soc*. **1986**, *108*, 1730.

(24) Nachbaur, L.; Nkinamubanzi, P.-C.; Nonat, A.; Mutin, J. C. *J. Colloid Interface Sci*. **1998**, *202*, (2), 261.